



# Hydraulic conductivity of GCL overlap permeated with saline solutions

Jackeline Gastelo, Dong Li, Kuo Tian<sup>\*</sup>, Burak F. Tanyu, F. Erol Guler

Department of Civil, Environmental and Infrastructure Engineering, George Mason University, Fairfax, VA 22030, USA

## ARTICLE INFO

### Keywords:

Geosynthetics  
Geosynthetic clay liner (GCL)  
Hydraulic conductivity  
GCL overlap  
Vertical flow  
Horizontal flow

## ABSTRACT

Hydraulic conductivity of the overlap region of two needle-punched sodium bentonite (Na-B) geosynthetic clay liners (GCLs) permeated with  $\text{CaCl}_2$  solutions under confining stresses of 20, 100, 250, and 500 kPa were evaluated. One of the GCLs consisted of a uniform layer of Na-B encapsulated between a nonwoven (NW) and a woven (W) geotextile, and the other one consisted of NW geotextiles on both sides. Supplemental bentonite was placed within the overlap region. Experiments were conducted with 10, 20, and 50 mM  $\text{CaCl}_2$  solutions representing dilute and aggressive leachates. The results indicate that in most of the scenarios there is a possibility that the flow is not completely vertical (meaning flow passes through the overlap region horizontally). As the confining stress increased, the horizontal flow through the overlap region for GCLs reduced effectively when permeated with deionized water and 10 mM  $\text{CaCl}_2$  solution, whereas the reduction of horizontal flow was limited to 20 mM and 50 mM  $\text{CaCl}_2$  solutions.

## 1. Introduction

Landfills are facilities designed for the containment of waste materials (Sharma and Lewis, 1994; Bouazza, 2002; Daniel, 2012; Parastar et al., 2017; Tian et al. 2016, 2019; Rowe, 2020). Typical liner systems for municipal solid waste (MSW) landfills in the U.S. are constructed with composite impermeable layers including a geomembrane underlain by a compacted clay layer (CCL) to prevent the migration of landfill leachates. A geosynthetic clay liner (GCL) may be used in lieu of a CCL as a sustainable alternative due to its low hydraulic conductivity (e.g.,  $<10^{-10}$  m/s), minimal thickness as it relates to saving air space in a landfill, and easy installation procedures (Daniel, 1993; Giroud et al., 1997; Shackelford et al., 2000; Scalia and Benson, 2010; Bradshaw et al., 2013, 2014; Setz et al., 2017; Bouazza et al., 2017; Tian et al., 2016, 2019).

GCLs consist of a thin layer of sodium bentonite (Na-B) clay (5–10 mm thick) sandwiched between two geotextiles where the geotextiles and the Na-B layers are held together by stitching, adhesives, and needle punching (Bouazza, 2002; Koerner, 2012; AbdelRazek and Rowe, 2019). The geotextile used in GCL can be nonwoven on both sides (NW-NW) or the combination of one nonwoven on one side and one woven on the other side (NW-W). The effectiveness of a GCL as a hydraulic barrier is controlled by the Na-B layer, which primarily consists of clay mineral montmorillonite. Montmorillonite has a high swelling capability after

hydration, which can eliminate the intergranular pore space and yield narrow and tortuous flow paths, resulting in a low hydraulic conductivity of GCLs (Jo et al., 2001, 2005; Lee et al., 2005; Kolstad et al., 2004; Bradshaw and Benson, 2014; Tian and Benson, 2014, Tian et al., 2016, Lu et al., 2018, Mukunoki et al., 2019). However, the swelling of Na-B can be inhibited when the GCL is exposed to saline solutions or leachates with high ionic strength or predominant polyvalent cations, which results in high hydraulic conductivity (Jo et al., 2001, 2005; Meer and Benson, 2007; Scalia et al., 2014; Setz et al., 2017; Tian et al., 2016, 2019; Chen et al., 2019; Zainab et al., 2021).

A majority of the previous studies focused on evaluating the hydraulic conductivity of the single GCL layer. However, considering the size of a landfill footprint, GCLs are always installed in the field where different sheets of GCLs are overlapped. This is because the typical width and length of GCL sheets range from 4 to 5.5 m and 30–60 m respectively compared to the average footprint of MSW landfill as 178,000 m<sup>2</sup> (EPA, 2001). The need to overlap GCL sheets in the field has also been recognized by the U.S. EPA, where the agency recommends a minimum overlap distance of 150 to 300 mm, depending on the particular product and site conditions (Daniel, 1993). The standard guide for installation of GCL (ASTM D6102) suggests that the minimum overlap between the two GCL panels should be 150 mm along the longitudinal direction, and the end-of-roll minimum overlap should be 500 mm. The minimum dimensions of the overlap are important to prevent the separation of

<sup>\*</sup> Corresponding author.

E-mail addresses: [jgastelo@masonlive.gmu.edu](mailto:jgastelo@masonlive.gmu.edu) (J. Gastelo), [dli8@gmu.edu](mailto:dli8@gmu.edu) (D. Li), [ktian@gmu.edu](mailto:ktian@gmu.edu) (K. Tian), [btanyu@gmu.edu](mailto:btanyu@gmu.edu) (B.F. Tanyu), [fguler@gmu.edu](mailto:fguler@gmu.edu) (F. Erol Guler).

<https://doi.org/10.1016/j.wasman.2022.12.028>

Received 12 May 2022; Received in revised form 4 December 2022; Accepted 23 December 2022

Available online 7 January 2023

0956-053X/© 2022 Elsevier Ltd. All rights reserved.

panels due to shrinkage of GCL (Thiel and Richardson, 2005; Rowe et al., 2010). A common method is placing Na-B in between the two GCLs at the overlap region with a minimum rate of 0.4 kg/m to seal the overlap area against horizontal flow through the geotextiles of the GCL. The Na-B added in the overlap region may be in a dry granular form or as a wet paste.

Previous studies conducted by Estornell and Daniel (1992), Cooley and Dainiel (1995), Daniel et al. (1997), Benson et al. (2004), Kendall and Austin (2014), Mazziari and Di Emidio (2015) have evaluated the performance of GCL overlaps. The first attempt in literature to evaluate the hydraulic conductivity of GCL overlap was made by Estornell and Daniel (1992). The particular NW-W GCL tested in their study had 5 kg/m<sup>2</sup> mass per unit area of bentonite. The rate of the supplemental bentonite that was placed in the overlap region was 0.4 kg/m. Two different overlap widths (75 and 150 mm) were evaluated at 9 kPa effective stress. The researchers presented that when the overlap width of NW-W GCL was reduced to 75 mm (half of the minimum recommended value of 150 mm), the hydraulic conductivity was 2.5 times higher than the value measured with 150 mm overlap. Estornell and Daniel (1992) suggested that the difference between the observations from the 75 and 150 mm overlaps could simply be the result of material variability. This research did not account for elevated effective (confining) stress conditions on GCL and the effect of different leachate compositions. Daniel et al. (1997) proposed a so-called flow box test set-up to evaluate the GCL overlap hydraulic conductivity. The test set-up was designed to measure vertical flow on both sides of the overlap and compare these values to the flow within the region where the GCL is overlapped. Comparative overlapped tests were conducted with and without the presence of bentonite in between the two GCLs at 6.2 kPa. Test results with bentonite seal were inconclusive as Daniel et al. (1997) stated that the cause for the incomplete self-sealing of the overlap is not known but may be related to the low confining pressure used in the tests. Weerasinghe et al. (2020) conducted experiments in a 1000 mm long and 500 mm wide flow box and evaluated the impact of overlap width of GCLs (e.g., 75 mm, 150 mm, and 300 mm) with supplemental bentonite when GCLs are permeated with tap water under two different confining stresses. Although the authors claimed that overlap width was the most significant parameter that affected the hydraulic performance, the presented results from the study showed the differences between smallest (75 mm) and largest (300 mm) overlaps to be by approximately a factor of 2 (i.e., normalized hydraulic flux from GCL overlaps with 75 mm was noted as  $1.97 \times 10^{-9} \text{ m}^3/\text{s}/\text{m}^2/\text{m}$ , with 150 mm was  $1.78 \times 10^{-9} \text{ m}^3/\text{s}/\text{m}^2/\text{m}$ , and with 300 mm was  $1.17 \times 10^{-9} \text{ m}^3/\text{s}/\text{m}^2/\text{m}$ ). This study shows that in terms of the flow, the overlap width may not have a great impact.

It is recognized in the literature that if the hydraulic conductivity of the region where the GCL pieces are overlapped is not watertight, these areas will potentially control the bulk hydraulic conductivity of the GCL layer installed in the landfill liner system. Considering that landfills contain different leachate compositions, the permeant solution that may be in contact with the GCL overlaps also plays an important role in the evaluations. However, as summarized above, the previous studies did not focus on specifically evaluating the integrity of the overlap regions based on different potential leachate compositions that could be seen in landfills. Therefore, the objective of the study presented in this manuscript was to evaluate the hydraulic performance of the overlap region of GCLs with supplemental bentonite. Experiments were conducted with 10, 20, and 50 mM CaCl<sub>2</sub> solutions representing dilute and aggressive leachates. A comparative test was conducted with two Na-B GCLs consisting of different geotextiles (NW-NW and NW-W) to determine the effect of geotextiles on the hydraulic performance of the overlap region. Tests were also conducted with DI water to serve as controls. Hydraulic conductivity tests were initially conducted at 20 kPa and then increased to 100, 250, and 500 kPa to mimic the stress conditions typically induced by the mass of the waste body in landfills. The study also included the hydraulic evaluation of the geotextiles alone to estimate the

flow through the geotextile extracted from GCL samples.

## 2. Methodology and materials

### 2.1. Geosynthetic clay liners (GCL) and permeant solutions

Tests were conducted with two commercially available needle-punched Na-B GCLs, i.e., one of the GCLs had nonwoven geotextile on both sides (NW-NW) and the other one had a nonwoven and a woven geotextile on each side (NW-W). The bentonite mass per unit area was 4.0 kg/m<sup>2</sup> for NW-NW GCLs and 3.96 kg/m<sup>2</sup> for NW-W GCLs. The swell index of bentonite extracted from GCLs were very comparable to each other. The bentonite from NW-W GCLs hydrated with DI water had a swell index of 36 mL/2g and from NW-NW GCLs had a swell index of 33 mL/2g. The comparative test results can evaluate whether the geotextile types used in the production of GCL make a difference in terms of the overlap behavior.

Tests were conducted with DI water (served as control tests) and 10, 20, and 50 mM CaCl<sub>2</sub> solutions. Solutions were prepared by dissolving powdered CaCl<sub>2</sub> salt in DI water. Ten and 20 mM CaCl<sub>2</sub> solutions were used to mimic the dilute to moderate leachate conditions respectively, and 50 mM CaCl<sub>2</sub> solution represented comparatively aggressive conditions (Jo et al., 2001, 2005; Scalia et al., 2014; Tian et al., 2019). The swell index of the bentonites extracted from NW-NW and NW-W GCLs in each testing solution was measured following the methods described in ASTM D5890 (ASTM, 20019).

### 2.2. Hydraulic conductivity test of GCL overlaps

The configuration of the laboratory set-up used to evaluate the hydraulic conductivity of the GCL overlaps using flexible wall permeameters is shown in Fig. 1. Tests were conducted with a conventional 152.4 mm diameter circular hydraulic chamber. This setup resulted in creating a 50.8 mm overlap condition between the two GCLs. This dimension is one-third of the minimum overlap requirements that are recommended in practice. However, it is important to point out that as indicated by Thiel and Richardson (2005) and Rowe et al. (2010), the minimum overlap dimensions for the GCLs are recommended based on preventing the separation of overlaps due to shrinkage of GCL installation in the field. Estornell and Daniel (1992) and Weerasinghe et al. (2020) also showed that the width of the GCL overlap has limited influence on the hydraulic performance of GCL overlaps. Considering that in the laboratory experiments, separation of overlaps due to shrinkage is not a concern, 50.8 mm is considered as a reasonable length to evaluate the effect of the GCL overlap on the hydraulic conductivity. However, it should be noted that the intent of this study was not to promote to reduce the previously established overlap lengths for the field applications, but it is intended to show that potentially the constructed overlaps may need to be further evaluated for their envisioned hydraulic performance (no flow conditions).

“Supplemental Bentonite method” was used to set up the GCL overlaps in this study. Most installation guidelines suggest the minimum application rate of bentonite for this type of scenario as 0.4 kg/m for the 150-mm overlap regions (EPA, 1993) (equal to 2.37 kg/m<sup>2</sup>). Considering the size of the overlap in this study, 18 g of Na-B were used in the overlap.

As can be seen from Fig. 1, the laboratory test set-up also included a set of NW geotextiles adjacent to the overlapped GCLs. These geotextiles were placed into the testing chamber to create a uniform sample thickness on both sides of the overlapped regions. The placed NW geotextiles were carefully selected to have a permeability that is larger than the permeability of the geotextiles within the GCL. This evaluation was conducted based on the manufacturer’s reported permittivity value of  $1.7 \text{ sec}^{-1}$  and thickness of 1.4 mm. Based on these reported values, the permeability of the NW geotextile that were used on both sides of the overlapped regions was calculated as  $2.4 \times 10^{-3} \text{ m}/\text{sec}$ .

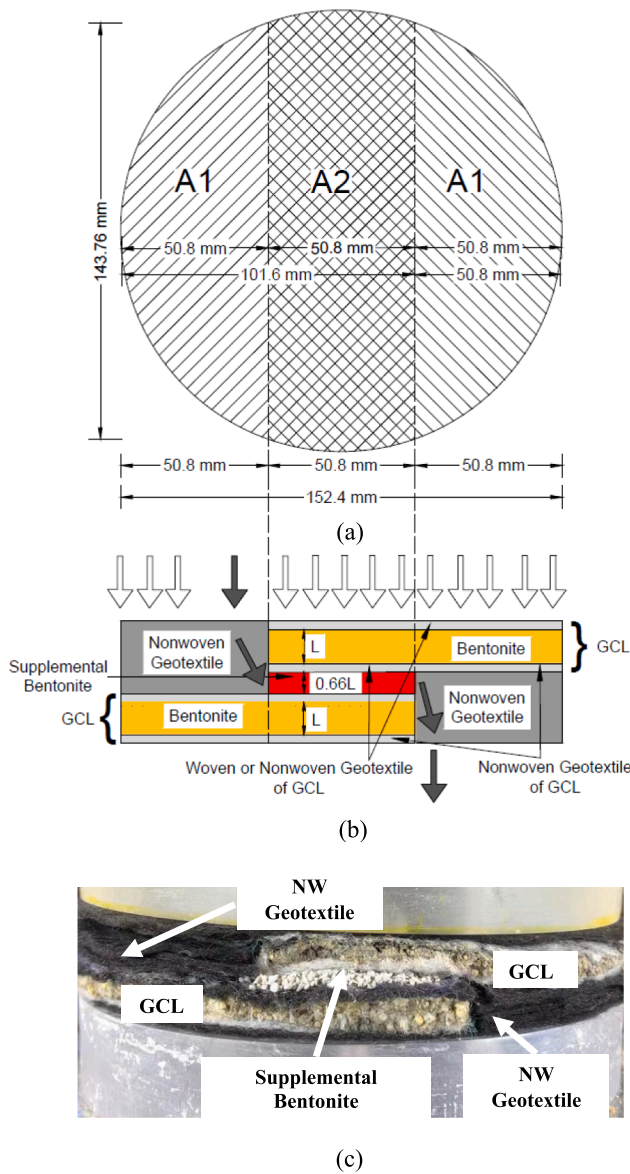


Fig. 1. (a) Plan view of GCL overlap specimens (b) Cross section views of GCL overlap specimens (c) Test set-ups of GCL overlap specimens. Note: The white arrow indicates the flow vertically passing through the GCLs. The black arrow indicates horizontal flow passing within the overlap region.

The hydraulic conductivity of GCL overlap was measured with a falling-head test using flexible-wall permeameters according to ASTM D6766. The hydration of the GCL specimens was achieved with effective stress of 20 kPa for 48 h with an average hydraulic gradient of 130. After hydration, the effluent line was opened. Fifty-milliliter burettes were used to contain the influent liquid and the effluent was collected using 60 mL HDPE bottles. All hydraulic conductivity tests were conducted until reaching hydraulic equilibrium and chemical equilibrium according to ASTM D6766. And then, incremental confining stress was applied to mimic the stress induced by the waste body (e.g., landfilling process). Control tests were conducted with single layer GCLs.

2.3. Transmissivity and permeability characteristics of the geotextiles of the GCL

The transmissivity and permeability characteristics of the geotextiles of GCLs were independently evaluated as part of this study to estimate the theoretical horizontal flow through geotextile layers at GCL overlap

region (Fig. 1b). To measure the in-plane flow capacity of the geotextiles, namely transmissivity, an experimental method was used with the set-up proposed by Abuel-Naga et al (2012). The detailed setup is discussed in the appendix (Fig. A1). The transmissivity values of the geotextiles were determined using constant head tests at effective stress of 20 kPa. The effective stress was then increased to 100, 250, and 500 kPa to determine the impact of stress on the transmissivity of geotextiles. For the transmissivity tests, the hydraulic gradient used was chosen as 10. The following equation was used to determine the transmissivity of geotextile ( $\theta$ ):

$$\theta = \frac{Q}{IP_{GTX}} \tag{1}$$

where  $\theta$  = transmissivity ( $m^2/s$ );  $Q$  = measured flow ( $m^3/s$ ),  $I$  = hydraulic gradient; and  $P_{GTX}$  = cross-sectional perimeter of the geotextile (m). In order to calculate the horizontal flow through geotextiles, the permeability of the geotextiles also had to be calculated. The following equation was used for this purpose:

$$k_{GTX} = \frac{\theta}{d} \tag{2}$$

where  $k_{GTX}$  = permeability of geotextile (m/s); and  $d$  = thickness of geotextile (m).

The thickness of the geotextiles was determined using a traditional consolidation cell that had the ability to apply different confining stress conditions and measure the corresponding deflections (i.e., changes in geotextile thickness). For this evaluation, ten layers of geotextile were stacked on top of each other. The thickness of both nonwoven and woven geotextiles was evaluated under confining stresses of 20, 100, 250, and 500 kPa. To determine the thickness of one layer of geotextile ( $d$ ), each measurement under each stress condition was divided by ten.

Table 1 presents the measured thickness of the geotextiles ( $d$ ), laboratory determined transmissivity ( $\theta$ ), and calculated in-plane permeability ( $k$ ) values corresponding to different effective stress conditions for different geotextiles (i.e.,  $k_{NW-GTX}$  for nonwoven geotextile and  $k_{W-GTX}$  for woven geotextile).

2.4. Bases of interpretation of the GCL overlap evaluations

2.4.1. Calculating hydraulic conductivity for each of the overlap GCL tests

Tests conducted in this study were based on falling head hydraulic conductivity procedures. The equation to calculate hydraulic conductivity ( $k$ ) based on such set-up is as follows:

$$k = \frac{aL}{At} \ln\left(\frac{h_1}{h_2}\right) \tag{3}$$

where  $a$  is the cross-sectional area of the reservoir containing the influent liquid ( $m^2$ );  $t$  is the elapsed time between the determination of

Table 1 Thickness, transmissivity and permeability of NW and W geotextiles at different effective stress conditions.

Effective stress (kPa)	NW geotextile			W geotextile		
	$d_{NW}$ (mm)	$\theta_{NW-GTX}$ ( $m^2/s$ )	$k_{NW-GTX}$ (m/s)	$d_W$ (mm)	$\theta_{W-GTX}$ ( $m^2/s$ )	$k_{W-GTX}$ (m/s)
20	1.280	$3.0 \times 10^{-7}$	$2.4 \times 10^{-4}$	0.689	$1.2 \times 10^{-7}$	$1.7 \times 10^{-4}$
100	0.932	$2.2 \times 10^{-7}$	$2.4 \times 10^{-4}$	0.549	$5.6 \times 10^{-9}$	$1.0 \times 10^{-5}$
250	0.707	$7.6 \times 10^{-8}$	$1.1 \times 10^{-4}$	0.349	$5.2 \times 10^{-11}$	$1.5 \times 10^{-7}$
500	0.591	$5.4 \times 10^{-9}$	$9.1 \times 10^{-6}$	0.229	$1.3 \times 10^{-11}$	$5.6 \times 10^{-8}$

Notes:  $d$ : thickness of geotextiles,  $\theta$ : transmissivity of geotextiles,  $k$ : permeability of geotextiles, NW: nonwoven geotextile of the GCL, and W: woven geotextile of the GCL.

$h_1$  and  $h_2$  (in seconds);  $h_1$  is the head loss across the specimen at time  $t_1$  (m); and  $h_2$  is the head loss across the specimen at time  $t_2$  (m),  $L$  is the thickness of the media that governs the flow (m),  $A$  is the cross-sectional area of the media that governs the flow ( $m^2$ ). Eq. (3) assumes that all of the flow occurs in the vertical direction. In the case of the overlap tests, this may or may not be true because there is a possibility that some of the flow may occur horizontally through the overlap region (see Fig. 1b).

In the overlap tests conducted in this study, the thickness of the media that governs the vertical flow is not uniform within the sample. This is because, in the zones where GCL is placed as a single layer and where GCL is overlapped, the thickness of the bentonite ( $L$ ) is different (see Fig. 1). Additionally, within the overlap region, the presence of supplemental bentonite also contributes to the thickness. To account for this, a mathematical term herein referred to as equivalent thickness ( $L_e$ ) is developed in this study.

Equivalent thickness ( $L_e$ ) can be calculated by taking into account that in each zone of the sample, the area and the thickness of the bentonite within the GCL can be determined. Fig. 1 shows three zones, two of which are designated as  $A_1$  for the areas that represent the zones for single GCLs and  $A_2$  for the area that represents the overlapped GCL zone. Each  $A_1$  area is  $0.005319 m^2$  and  $A_2$  area is  $0.007594 m^2$ . The thickness of the bentonite in the  $A_1$  region is equivalent to the thickness of the single layer of bentonite ( $L$ ), herein referred as  $L_1$ . In the  $A_2$  region, there are two bentonite layers and supplemental bentonite. The mass per unit area of supplemental bentonite used in this study was  $2.37 kg/m^2$ . For one GCL (that has a thickness of  $L_1$ ), the mass per unit area of the bentonite is reported as  $3.6 kg/m^2$  by the manufacturer. Therefore, it is estimated that the thickness of the bentonite to satisfy the  $2.37 kg/m^2$  mass per unit area, the thickness of the bentonite has to be approximately 65.8% of  $L_1$  (or  $0.66 L_1$ ). Based on this estimation, the overall thickness of the overlap region with the supplemental bentonite would equate to  $2 \times L_1 + 0.66 L_1 = 2.66 L_1$ .

Therefore, the total flow through GCL that passes through the total area of  $Q_{Total}$  can be calculated as shown in Eq.4:

$$Q_{Total} = 2 \times Q_1 + Q_2 \tag{4}$$

where  $Q_{Total}$  is the total flow through GCL overlap specimen,  $Q_1$  is the flow through  $A_1$  region, and  $Q_2$  is the flow through  $A_2$  region. The equation can be re-written as Eq. (5).

$$k_a \frac{\Delta H}{L_e} A = 2k \times \frac{\Delta H}{L_1} A_1 + k \times \frac{\Delta H}{L_2} A_2 \tag{5}$$

where  $k_a$  is the apparent hydraulic conductivity of overlap specimen,  $L_e$  is the equivalent thickness of GCL overlap samples.  $L_e$  can be determined as a function of  $L_1$  as  $L_e = 1.35 L_1$ .  $L_e$  was used for the tests conducted with the supplemental bentonite scenario.

Once the term  $L_e$  is established for each testing condition, this parameter was used to replace the  $L$  in Eq. (3) to calculate the vertical hydraulic conductivity for each of the overlap GCL tests.

2.4.2. Total, vertical and horizontal flow scenarios through the GCL overlap region

For GCL overlap region, two possible flow scenarios may occur at the overlap region (vertical vs. horizontal flow) (Fig. 1b). Analyzing the hydraulic conductivity of GCL overlap with Eq. (3) cannot provide insight about the proportions of the total flow that may be due to vertical or horizontal flow. Therefore, tests were conducted with single layer GCL to different  $CaCl_2$  solutions to estimate the vertical flow, while theoretical horizontal flow through geotextiles was also measured and predicted.

To interpret the test results and to estimate the proportions of the flow that may be due to vertical versus horizontal scenarios, the following formulations were used with the assumption that in all cases the hydraulic head ( $\Delta H$ ) was assumed as constant and 1 m.

Total flow calculated from each overlap test (not differentiating between horizontal and vertical flow) ( $Q_{Total}$ ):

$$Q_{Total} = k \times \frac{\Delta H}{L_e} \times A_{Total} \tag{6}$$

where  $k$  is determined from Eq. (3),  $L_e$  is determined from Eqs. 4 or 5, and  $A_{Total}$  is calculated as  $2A_1 + A_2$  (Fig. 2).

Flow through single (1) GCL (representing the purely vertical flow condition):

$$Q_{Vert-GCL} = k \times \frac{\Delta H}{L_1} \times A_{Total} \tag{7}$$

where  $k$  is determined from experiments conducted with single GCL,  $L_1$  is the thickness of the bentonite within the tested single GCL, and  $A_{Total}$  is the cross-sectional area of the GCL sample.

Flow within the planes of the GCL geotextiles in the overlap tests (representing the maximum possible calculated horizontal flow condition through geotextiles without bentonite extrusion) ( $Q_{Horz-NW+NW}$ ,  $Q_{Horz-NW+W}$ ):

The horizontal flow may take place either within the plane of the

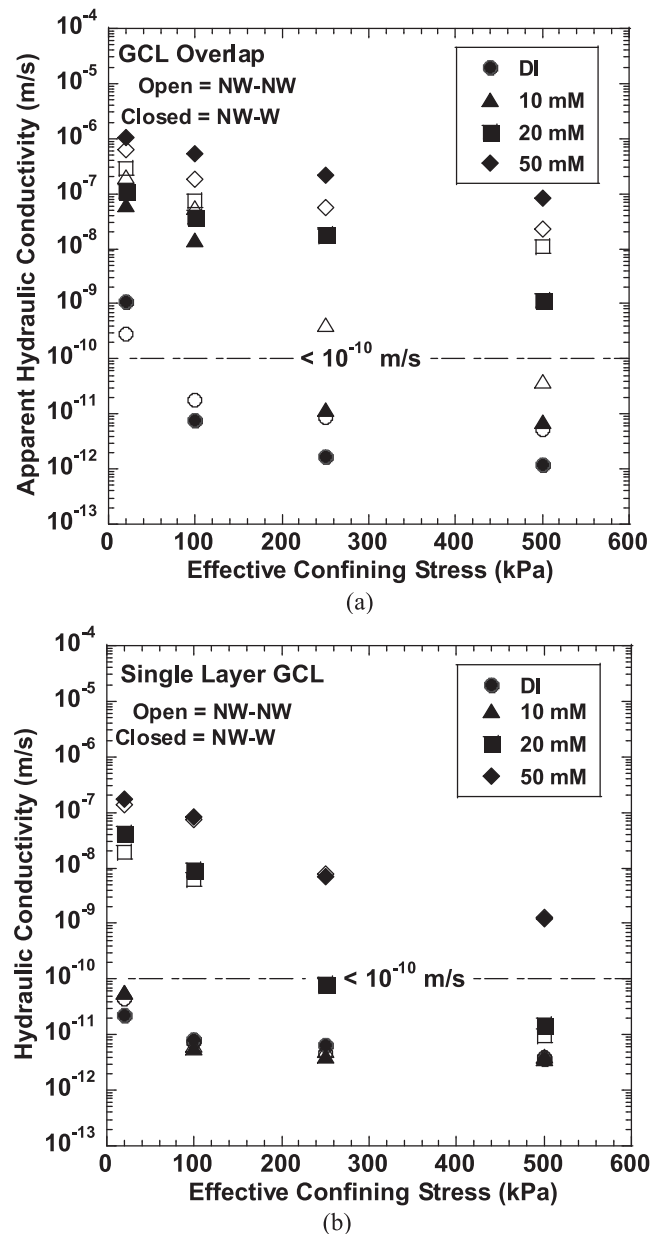


Fig. 2. Hydraulic conductivity of GCL overlaps (a) and single layer GCL (b) as a function of different effective stress and permeant solutions.

geotextile or the bentonite in between the two GCLs. The bentonite may be placed during construction, which is expected to infuse into geotextiles as the effective confining stress increases. As shown in Table 1, the permeability of the geotextiles that were intact to the GCLs was in the range of  $10^{-4}$  m/s under 20 kPa effective stress conditions. Even under 500 kPa stress conditions, the permeability still stayed within the range of  $10^{-8}$  m/s (Table 1). When compared with the typical hydraulic conductivity of bentonite (e.g.  $< 10^{-10}$  m/s) (Tian et al., 2016), the ability of the geotextiles to permeate fluid is significantly higher. Thus, when determining the calculated horizontal flow through the overlap region, the evaluations in this study have focused on the horizontal flow being through the geotextile and not through the supplemental bentonite that is present in-between the two GCLs at the overlap zone.

In the case where the flow occurs through both of the geotextiles, the horizontal flow is estimated as:

$$Q_{Horz-NW+NW} = 2 \times k_{NW-GTX} \times \frac{\Delta H}{l_{overlap}} \times A_{NW-GTX} \quad (8)$$

$$Q_{Horz-NW+W} = k_{W-GTX} \times \frac{\Delta H}{l_{overlap}} \times A_{W-GTX} + k_{NW-GTX} \times \frac{\Delta H}{l_{overlap}} \times A_{NW-GTX} \quad (9)$$

where  $Q_{Horz-NW+NW}$  represents the maximum calculated horizontal flow through both clean NW geotextiles (e.g., without bentonite intrusion) for the NW-NW GCL overlaps with the supplemental bentonite method (Eq. (8)),  $Q_{Horz-NW+W}$  represents the maximum calculated horizontal flow through both W and NW geotextiles for the NW-W GCL overlaps (Eq. (9)).  $l_{overlap}$  is the length of the overlap region, equal to 50.8 mm.  $k$  is the hydraulic conductivity of NW or W geotextiles (shown in Table 1). The cross-sectional areas ( $A_{NW-GTX}$  or  $A_{W-GTX}$ ) shown in Eqs.8 and 9 were estimated as a function of the geotextile thicknesses under different confining stress conditions as  $0.1437 \times d_{NW \text{ or } W}$  (obtained from Table 1) ( $m^2$ ).

### 3. Results and discussions

#### 3.1. Hydraulic conductivity test results

Hydraulic conductivity of GCL overlaps (apparent hydraulic conductivity) and single layer GCL tested with different saline solutions (e.g., 10, 20, 50 mM  $CaCl_2$ ) and DI water under 20, 100, 250, and 500 kPa confining stress are shown in Fig. 2. An example of the temporal behavior of the apparent hydraulic conductivity of GCL overlaps as a function of confining stress is shown in Appendix (Fig. A2). Regardless of the GCL type and the permeant solution, as the confining stress conditions are increased, the apparent hydraulic conductivity in each test decreased. This observation as it relates to trends supports the previous observation from single GCLs that were tested for hydraulic conductivity (Bradshaw et al., 2016, Li et al., 2021).

At 20 kPa confining stress condition, none of the overlap tests, regardless of the type of GCL and the solution, had apparent hydraulic conductivity  $< 1 \times 10^{-10}$  m/s (Fig. 2a). When the effective stress increased to 100 kPa, for GCL overlaps permeated with DI water permeability decreased to  $7.7 \times 10^{-12}$  to  $1.8 \times 10^{-11}$  m/s for NW-W and NW-NW samples respectively (Fig. 2a). As the confining stress increased to 250 kPa, the apparent hydraulic conductivity of NW-W and NW-NW GCL overlaps to 10 mM  $CaCl_2$  solution also met the minimum regulatory requirement. All other test results with 20 and 50 mM  $CaCl_2$  solutions showed unacceptable apparent hydraulic conductivity even under 500 kPa confining stress conditions (Fig. 2a).

To be able to estimate the flow through a single layer of GCL and to compare the results with the overlap tests, hydraulic conductivity tests were also conducted on single GCLs under different vertical pressures and with the same permeant solutions that were used in GCL overlap tests (Fig. 2b). The single GCL hydraulic conductivity tests also showed that there was little difference in hydraulic conductivity between the

GCLs with NW-NW and NW-W geotextiles. This supports the theory that in single GCL tests where the flow is perpendicular to the direction of the GCL, the overall hydraulic conductivity of the GCL is controlled by the Na-B layer. Single layer GCLs showed lower hydraulic conductivity than that of the overlap tests at the same testing condition. When the permeability of a single GCLs is compared to those of GCL overlaps permeated with the same leachate and at the same effective confining stress, it is seen that there is a significant difference. For example, hydraulic conductivity of single GCL was  $1.0 \times 10^{-10}$  m/s when permeated with DI water and 10 mM  $CaCl_2$  at 20 kPa, whereas for the same permeant solutions, the flow within the GCL overlaps was in the order of  $2.8 \times 10^{-10}$  to  $1.1 \times 10^{-9}$  m/s (much higher apparent hydraulic conductivity). When permeated with 20, 50 mM  $CaCl_2$ , the osmotic swelling of Na-B in the GCLs was inhibited, leading to large intergranular pore space and high hydraulic conductivity of single layer GCLs ( $> 10^{-10}$  m/s). The hydraulic conductivity of single GCL was still higher than that of GCL overlaps when permeated with 20, 50 mM  $CaCl_2$ . Additionally, when permeated with 20 mM  $CaCl_2$  solutions at 500 kPa effective confining stress, the single hydraulic conductivity of single GCLs (e.g.,  $1.5 \times 10^{-11}$  to  $9.5 \times 10^{-12}$  m/s) were approximately two to three orders of magnitude lower than those of GCL overlaps (e.g.,  $1.1 \times 10^{-9}$  to  $1.1 \times 10^{-8}$  m/s). Those observations indicate that horizontal flow through the geotextile occurred through the GCL overlaps. However, the comparison of the performance based on hydraulic conductivity values is not enough to quantify such differences. Such comparison requires to distinguish between the total, horizontal, and vertical flows within a GCL overlap test. Results associated with this comparison are presented in the subsequent section.

#### 3.2. Comparison of Total, Horizontal, and vertical flow

The total flow from GCLs could be obtained based on Eq. (6) from the hydraulic conductivity values obtained from GCL overlap tests. However, these flow values do not differentiate whether the flow has taken place vertically, horizontally, or both. Eq. (7) provides the total flow from single GCLs. Such information predominantly indicates the conditions where the flow is vertical. To have a clue about the horizontal flow conditions, the permeability of the geotextiles extracted from GCLs also had to be known. Results of the hydraulic conductivity tests conducted to measure the transmissivity of NW and W geotextiles are presented in Table 1. The results showed that as the confining stress increased the transmissivity of the geotextiles decreased (as expected). In the case of NW geotextile, the decrease is from  $3.0 \times 10^{-7}$  to  $5.4 \times 10^{-9}$   $m^2/s$  and for W geotextile, the decrease is from  $1.2 \times 10^{-7}$  only to  $1.2 \times 10^{-11}$  m/s. The measured transmissivity values under different vertical pressures were then used with the help of Eq. (2), to calculate the hydraulic conductivity of the W and NW geotextiles. Considering that the chemistry of the permeant solutions does not influence the amount of flow through geotextiles, calculations based on Eqs. (8) thru 9 could be compared against the values obtained from Equations (6) and (7) to evaluate the conditions governed by horizontal vs. vertical flow conditions. Such comparison for each effluent condition is presented below.

In each comparison, calculated maximum horizontal flow amounts were compared against the flow from single GCLs and total flow from overlapped GCLs. This comparison provides insight regarding whether the total flow shows indicatives of the calculated horizontal flow or vertical flow. The total, horizontal and vertical flow of GCL overlaps are calculated based on a one-meter constant head. In this comparison, the maximum hydraulic conductivity of  $10^{-10}$  m/s threshold has also been converted into the flow based on one-meter constant head and 150 mm diameter specimen. This threshold flow is calculated as  $3.0 \times 10^{-10}$   $m^3/s$ .

##### 3.2.1. Tests with DI water

Fig. 3 presents the flow rate of GCLs tested with DI water. At 20 kPa,

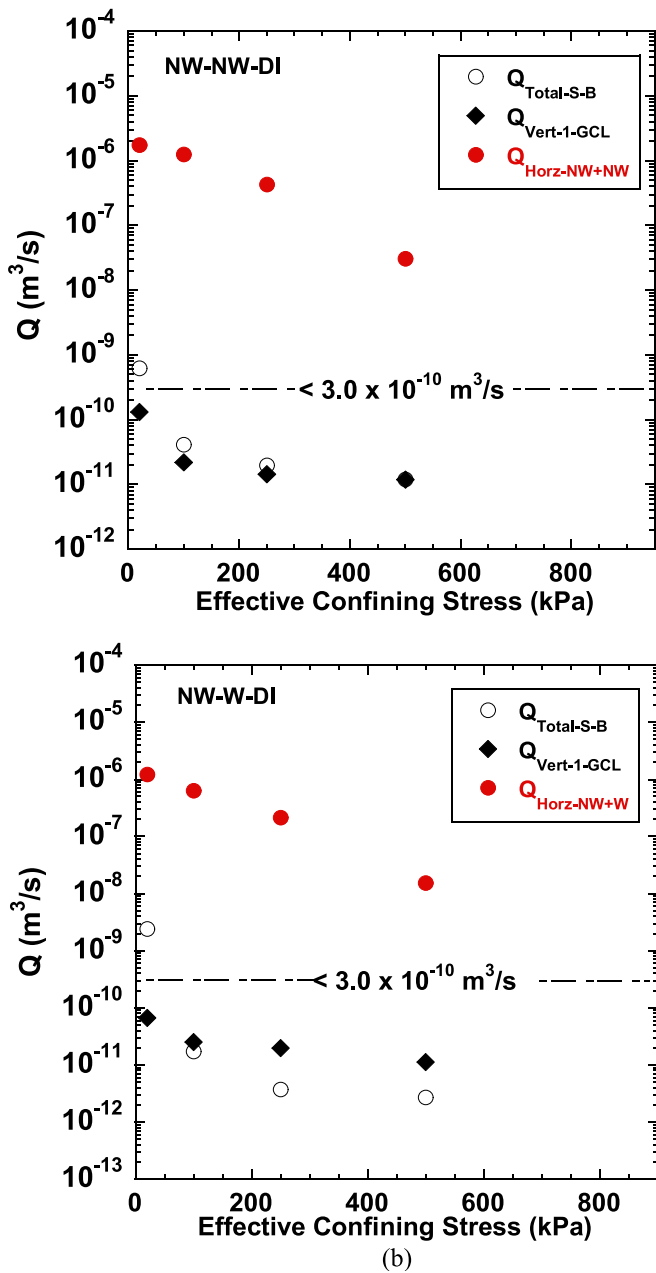


Fig. 3. Total, horizontal, and vertical flow of GCL overlaps to DI water as a function of effective confining stresses: (a) NW-NW, (b) NW-W.

the results show that the total flow of NW-NW GCL overlaps were close to the flow from single GCL tests (Fig. 3a), indicating that there was minimal horizontal flow. All total flow rates remained below the  $3 \times 10^{-10} \text{ m}^3/\text{s}$  threshold at elevated confining stress, illustrating that supplemental bentonite overlap methods provide a good overlap for NW-NW GCLs when permeated with DI water. Similar behavior was observed for the NW-W GCL (Fig. 3b). This is most likely because the Na-B swells highly in DI water (36 mL/2 g) and intrudes into the NW geotextile sufficiently to significantly reduce the horizontal flow through the geotextile. Similar findings were also concluded by Di Emidio et al. (2008). As the effective confining stress increased, the flow of GCL overlaps kept decreasing, indicating horizontal flow through geotextiles may further decrease, because the Na-B is pressurized to the geotextile more tightly and therefore block the horizontal flow after being consolidated.

3.2.2. Test with 10 mM CaCl<sub>2</sub> solution

Fig. 4 presents the flow rates when the GCLs were tested with 10 mM CaCl<sub>2</sub> solution. The flow rate of single GCL to 10 mM CaCl<sub>2</sub> mM solution was similar to that of single GCL to DI water ( $1.2 \times 10^{-11} \text{ m}^3/\text{s}$  vs.  $2.3 \times 10^{-10} \text{ m}^3/\text{s}$ ) at 20 kPa effective confining stress. However, the total flow of NW-NW and NW-W GCL overlaps permeated with 10 mM CaCl<sub>2</sub> were higher than those to DI water at low-stress condition (e.g., 20 kPa), indicating more horizontal flow through the geotextiles. The reason for this is possible that although the bentonite between the geotextiles swells and intrudes into the geotextiles, horizontal flow cannot be blocked completely due to the reduction of swelling of Na-B (e.g., 36 mL/2 g in DI water vs. 22–24 mL/2 g in 10 mM CaCl<sub>2</sub>).

Since the vertical flow is much lower than the horizontal flow, the

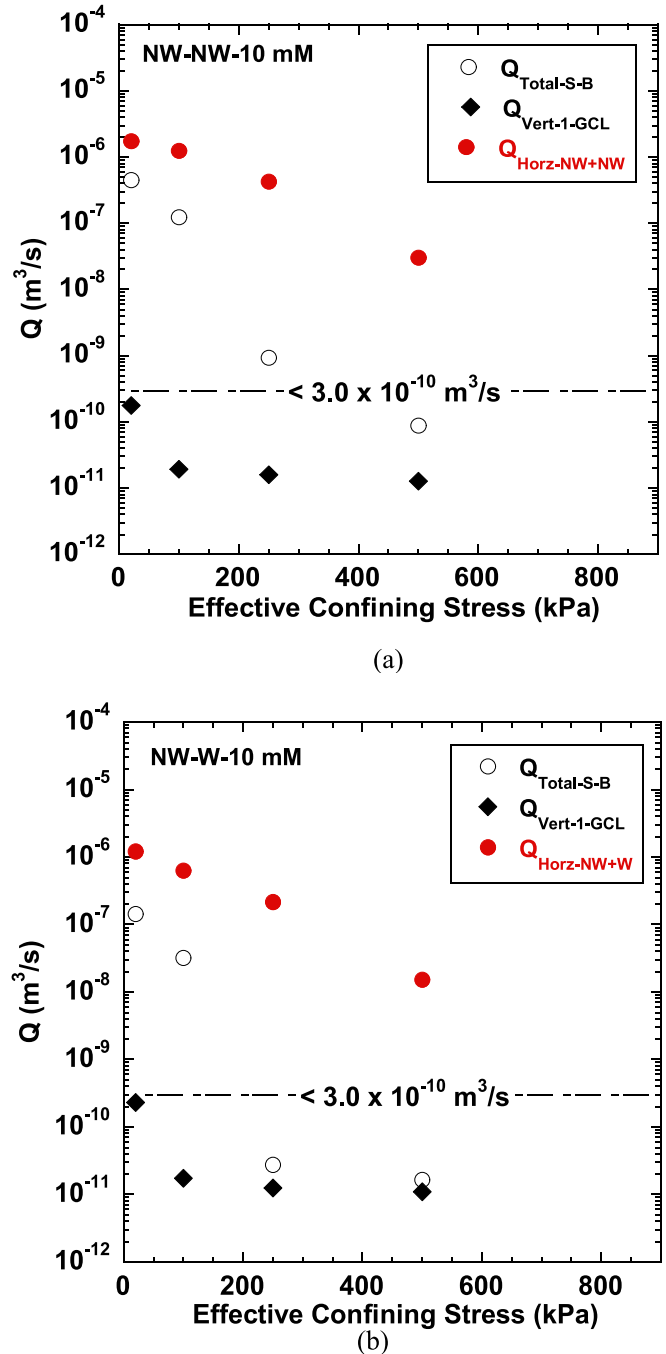


Fig. 4. Total, horizontal, and vertical flow of GCL overlaps to 10 mM CaCl<sub>2</sub> solution as a function of effective confining stresses: (a) NN-NW, (b) NW-W.

total flow of overlap GCLs is controlled by the horizontal flow through geotextiles. The dye test was conducted with NW/NW GCL overlap using supplemental bentonite to determine preferential flow path (horizontal vs. vertical) using the method developed by Scalia and Benson (2010). The test was conducted at 20 kPa confining stress and the cross-section is shown in Fig. 5. The bentonite layer of GCL and supplemental bentonite layer remained in their original light gray color. In contrast, the geotextiles of GCL turned pink color after permeation. This observation indicates that the flow predominately occurred in the geotextile layer of the GCL overlap region, which illustrates the horizontal flow concept in this study as described in Fig. 1b.

The total flow of GCL overlap decreased slightly as the effective confining stress increased from 20 kPa to 100 kPa (Fig. 4a and b), indicating that although the geotextile stick to the bentonite more closely at 100 kPa, and reduce the horizontal flow because of the consolidation, the total flow of overlap GCLs was still mainly controlled by the horizontal flow (geotextile). When the effective stress increased from 100 to 250 kPa, the total flow of NW-NW and NW-W GCL overlap decreased sharply. This again is interpreted as the geotextiles adhering to the bentonite more closely and the reduction of geotextiles' thickness at 250 kPa. Meanwhile, more bentonite may be intruded into the geotextiles to block more pore space at higher stress levels. The combination of all these effects decreases the portion of the horizontal flow to the total flow of GCL overlaps, leading to shifting from horizontal flow control to vertical flow control scenario. The hydraulic conductivity of single NW-W and NW-NW GCLs showed similar hydraulic conductivity when permeated with CaCl<sub>2</sub> solution as shown in Fig. 2(b). The total flow of NW-W GCL overlaps was lower than that of NW-NW GCL overlaps at 250 kPa and 500 kPa, which may be attributed to the lower transmissivity of W geotextiles in comparison with NW geotextiles.

3.2.3. Test with 20 mM CaCl<sub>2</sub> solution

Fig. 6 presents the flow values when the GCLs were tested with 20 mM CaCl<sub>2</sub> solution. The results show a similar trend with the specimens permeated with 10 mM CaCl<sub>2</sub> but somewhat more pronounced. The test results of NW-NW and NW-W GCL overlaps were very similar in terms of total flow. With increasing effective stress, the total flow measured from the NW-NW and NW-W GCL overlaps specimens deviated from the flow of single GCLs and became closer to the theoretical horizontal flow through the geotextiles of the overlap, especially at 250 and 500 kPa confining stress. This can be explained by the fact that the consolidation of the Na-B in GCL reduced the vertical flow as the result of a single GCL, but the reduction in horizontal flow was limited when permeated with 20 mM CaCl<sub>2</sub>. This is because swelling of Na-B was inhibited by the 20 mM CaCl<sub>2</sub> solution (17 mL/2g) and resulted in limited amount of Na-B intruding into the nonwoven geotextile to block the horizontal flow.

3.2.4. Test with 50 mM CaCl<sub>2</sub> solution

Fig. 7 presents the flow rates of GCLs permeated with 50 mM CaCl<sub>2</sub> solution. This permeant solution is considered aggressive and tests

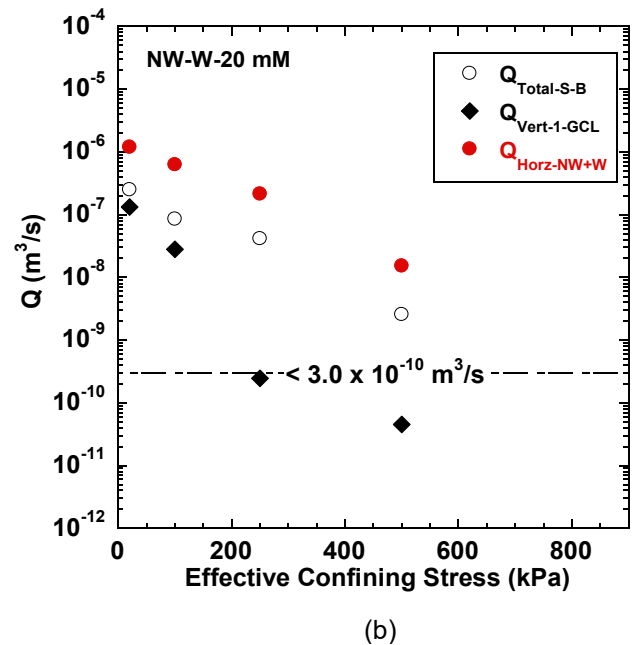
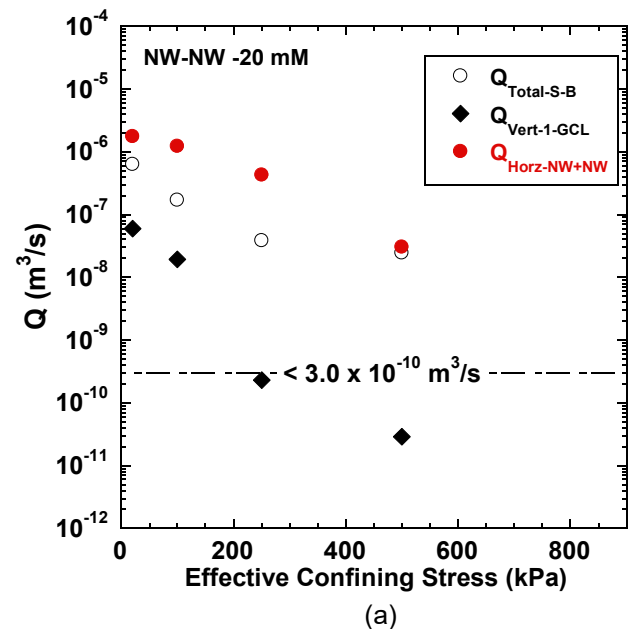


Fig. 6. Total, horizontal, and vertical flow of GCL overlaps to 20 mM CaCl<sub>2</sub> solution as a function of effective confining stresses: (a) NN-NW, (b) NW-W.

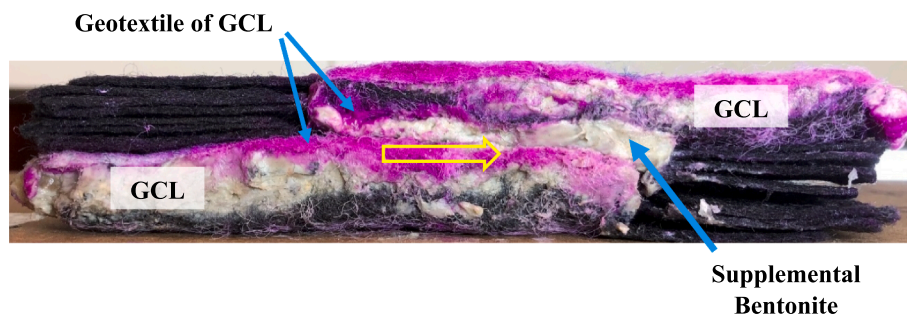


Fig. 5. Cross-section showing preferential flow (bold yellow arrow) through geotextiles of NW/NW GCL overlap with supplemental bentonite permeated with 10 mM CaCl<sub>2</sub> solution at 20 kPa confining effective stress. (For interpretation of the references to color in this figure legend, the reader is referred to the web version of this article.)

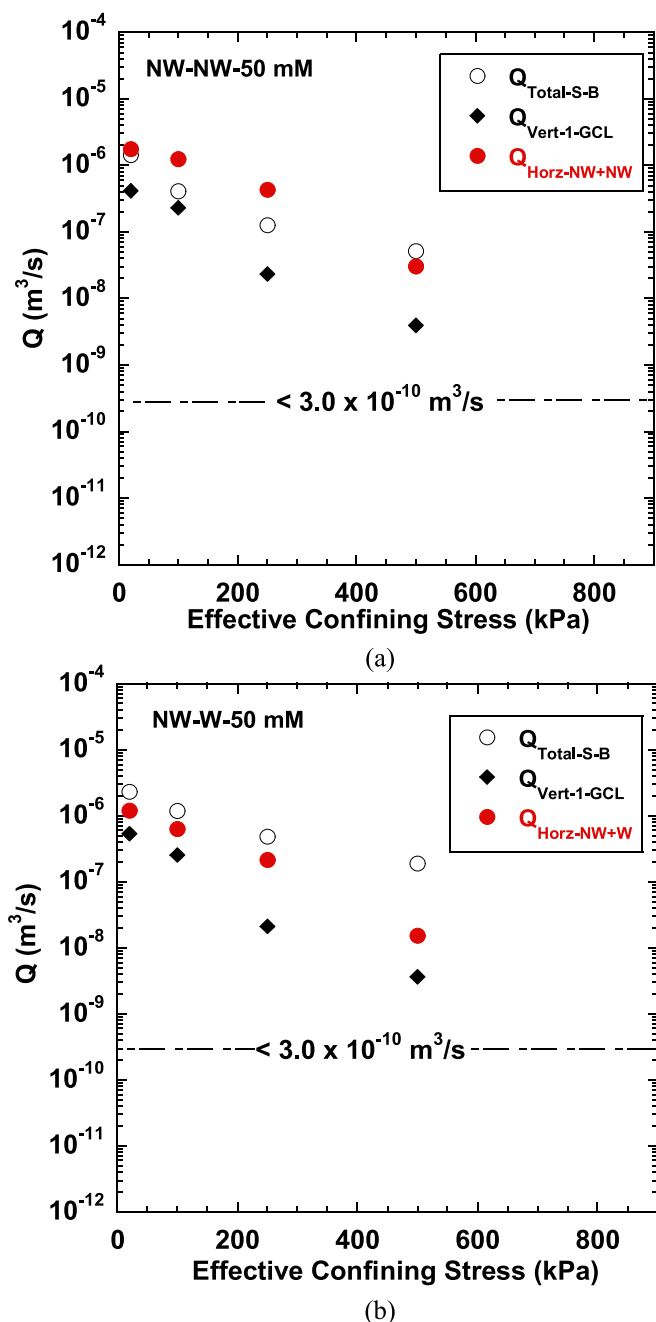


Fig. 7. Total, horizontal, and vertical flow of GCL overlaps to 50 mM  $\text{CaCl}_2$  solution as a function of effective confining stresses: (a) NN-NW, (b) NW-W.

conducted with single GCLs can be interpreted as controls. In both NW-NW and NW-W GCLs, the total flow conditions were significantly above the so-called threshold flow values ( $<3 \times 10^{-10}$   $\text{m}^3/\text{s}$ ). This observation is not surprising considering that Na-B GCL cannot maintain low hydraulic conductivity ( $<10^{-10}$   $\text{m/s}$ ) due to the suppression of swelling of Na-B in 50  $\text{CaCl}_2$  mM (11 mL/2 g), as concluded in Jo et al. (2001), Scalia et al. (2014).

In the case of NW-NW GCLs, the calculated horizontal flow of geotextiles, vertical flow of single GCL, and total flow of GCL overlap specimens decreased as effective confining stress increased. The total flow of GCL overlaps was closer to the horizontal flow (single GCL), indicating that both horizontal and vertical flow contributed to the total flow. When the effective stress increased to 250 kPa and 500 kPa, the difference between the total flow of GCLs overlaps and the vertical flow of single GCL became larger, indicating the total flow of GCL overlaps

was controlled more by the horizontal flow (geotextile). At 500 kPa, the  $Q_{\text{Total-S-B}}$  was higher than the calculated maximum flow through geotextiles ( $Q_{\text{Horz-NW+NW}}$ ), indicating that some of the horizontal flow may also occur through the supplemental bentonite layer between the two GCLs. The supplemental bentonite layer appears to not be able to prevent the horizontal flow completely due to the suppression of swell of Na-B in 50 mM  $\text{CaCl}_2$  solution (e.g., 10 to 11 mL/2 g).

In the case of NW-W GCL overlaps, the GCL had a higher flow than that of a single GCL, illustrating that horizontal flow occurred through the GCL overlap region. The total flow through the NW-W GCL overlap with the supplemental bentonite method was higher than the calculated horizontal flow through both NW and W geotextiles, which may be interpreted as horizontal flow also occurred at the supplemental bentonite layer. A similar interpretation was also discussed for the NW-NW GCL overlaps under 500 kPa confining stress.

#### 4. Summary and conclusions

This study was conducted to evaluate the hydraulic performance of GCL overlaps that are prepared using the supplemental bentonite method. Na-B GCLs consisting of different geotextile combinations (NW-NW and NW-W) were used. GCLs were permeated with DI water and  $\text{CaCl}_2$  solutions.  $\text{CaCl}_2$  solution concentrations were selected as 10, 20, and 50 mM to simulate dilute and aggressive leachates. Hydraulic conductivity tests were conducted at 20, 100, 250, and 500 kPa effective confining stress to mimic the effect of the mass of the waste body. To determine the efficiency of the overlaps in terms of vertical and horizontal flow conditions, supplemental tests were also conducted with single GCL and geotextiles alone. Hydraulic conductivity tests with single GCLs were evaluated to assess the vertical flow under the same test conditions as followed for the GCL overlap tests. Hydraulic conductivity tests with NW and W geotextiles extracted directly from the GCL samples were used to assess transmissivity. This information was used in estimating the calculated horizontal flow through the geotextile component of the GCLs within the overlap region.

The following conclusions are based on the findings of this study:

- 1) Comparative hydraulic tests were conducted with NW-NW GCL and NW-W GCL overlaps. Results were similar to each other at the same testing conditions.
- 2) The flow through overlap setup permeated with DI water appeared to be similar to the flow of single layer GCL at the same test condition, especially at higher confining stresses. This indicates that the horizontal flow through the GCL overlaps was blocked effectively when GCLs are permeated with DI water. However, in the case of tests conducted with saline solution, the total flow obtained from the tests conducted with the GCL overlap setup was higher than that of single layer GCL. This indicates the appearance of horizontal flow.
- 3) As the  $\text{CaCl}_2$  concentration of the saline solution increases, the possible horizontal flow path appears to also be changing. When the permeant solution is less aggressive in terms of  $\text{CaCl}_2$  concentration and when minimum vertical stress is applied (such as in the case of 10 mM  $\text{CaCl}_2$  solution at 20 kPa test), the horizontal flow path mainly occurs through the carrier geotextiles (NW or W) on GCL overlaps. When permeated with aggressive saline solutions (50 mM), horizontal flow may also occur through the supplemental bentonite layer in between the two overlapped GCLs.
- 4) The horizontal flow through GCL overlap was reduced as the effective confining stress increases. However, such affect was more pronounced in tests conducted with less aggressive permeant solutions. For example, when permeated with 10 mM  $\text{CaCl}_2$  solution, the horizontal flow through the overlap region for GCLs were blocked effectively for the confining stresses at 250 and 500 kPa. For the same vertical stress conditions, when tests were conducted with 20 mM and 50 mM  $\text{CaCl}_2$  solutions, the horizontal flow was reduced, but not blocked.

Although the overlap zones in the field applications constitute only a small percentage of the total coverage area, this study indicates that those zones deserve a more detailed evaluation as they may constitute weaker zones in terms of flow. It is undoubtedly agreed that further studies are needed to confirm that the observations noted in this study hold true when the overlap region is extended to 150 mm. This is because the effects of sample size may affect the test results.

### Declaration of Competing Interest

The authors declare the following financial interests/personal relationships which may be considered as potential competing interests: Kuo Tian reports financial support was provided by Geosynthetic Institute.

### Data availability

Data will be made available on request.

### Acknowledgments

Financial support for parts of this study described in this article was provided by Geosynthetic Institute (GSI). The conclusions and recommendations listed in this article are those of the authors and do not reflect the opinions or policies of GSI. Authors greatly appreciate these financial and in-kind supports.

### Appendix A. Supplementary data

Supplementary data to this article can be found online at <https://doi.org/10.1016/j.wasman.2022.12.028>.

### References

- AbdelRazek, A.Y., Rowe, R.K., 2019. Interface transmissivity of conventional and multi-component GCLs for three permeants. *Geotext. Geomembranes* 47 (1), 60–74.
- Abuel-Naga, H.M., Bouazza, A., Lalot, E., 2012. On measuring the hydraulic transmissivity of the geotextile cover of geosynthetic clay liners. *Geosyn. Int.* 19 (4), 319–323.
- ASTM D 5890, 2019. Standard test method for swell index of clay mineral component of geosynthetic clay liners. ASTM International, West Conshohocken, Pennsylvania, USA.
- ASTM D 6102, 2020. Standard Guide for Installation of Geosynthetic Clay Liners. ASTM International, West Conshohocken, Pennsylvania, USA.
- ASTM D 6766, 2018. Standard Test Method for Evaluation of Hydraulic Properties of Geosynthetic Clay Liners Permeated with Potentially Incompatible Aqueous Solutions. ASTM International, West Conshohocken, Pennsylvania, USA.
- Benson, C.H., Jo, H.Y., Abichou, T., 2004. Forensic analysis of excessive leakage from lagoons lined with a composite GCL. *Geosynth. Int.* 11 (3), 242–252.
- Bradshaw, S.L., Benson, C.H., Scalia, J., 2013. Hydration and Cation Exchange during Subgrade Hydration and Effect on Hydraulic Conductivity of Geosynthetic Clay Liners. *J. Geotech. Geoenviron. Eng.* 139 (4), 526–538.
- Bradshaw, S.L., Benson, C.H., 2014. Effect of municipal solid waste leachate on hydraulic conductivity and exchange complex of geosynthetic clay liners. *J. Geotech. Geoenviron. Eng.* 140 (4), 04013038.
- Bradshaw, S.L., Benson, C.H., Rauon, T.L., 2016. Hydraulic conductivity of geosynthetic clay liners to recirculated municipal solid waste leachates. *J. Geotech. Geoenviron. Eng.* 142 (2), 1–12.
- Bouazza, A., 2002. Geosynthetic clay liners. *Geotext. Geomembranes* 20 (1), 3–17.
- Bouazza, A., Ali, M.A., Gates, W.P., Rowe, R.K., 2017. New insight on geosynthetic clay liner hydration: the key role of subsoils mineralogy. *Geosynth. Int.* 24 (2), 139–150.
- Chen, J.N., Salihoglu, H., Benson, C.H., Likos, W.J., Edil, T.B., 2019. Hydraulic Conductivity of Bentonite-Polymer Composite Geosynthetic Clay Liners Permeated with Coal Combustion Product Leachates. *J. Geotech. Geoenviron. Eng.* 145 (9), 1–12.
- Cooley, B.H., Daniel, D.E. 1995. Seam performance of overlapped geosynthetic clay liners. In *Proceedings of Geosynthetics '95*, Nashville, Tenn., 21–23 February 1995. Industrial Fabrics Association International, St. Paul, Minn. pp. 691–705.
- Daniel, D.E., 1993. Landfills and impoundments. In *Geotechnical practice for waste disposal*, Springer, Boston, MA.
- Daniel, D.E., Bowders, J.J., Gilbert, R.B., 1997. Laboratory hydraulic conductivity testing of GCLs in flexible-wall permeameters. In *Testing and acceptance criteria for geosynthetic clay liners*. ASTM Spec. Tech. Publ. 1308, 208–228.
- Daniel, D.E., 2012. *Geotechnical Practice for Waste Disposal*. Springer, Boston, MA, USA.
- Di Emidio, G., Mazzieri, F., Van Impe, P.O., Van Impe, W.F., 2008. Hydraulic conductivity performance of a Dense Prehydrated GCL overlap permeated with sea water. *Proceedings 1st Pan American Geosynthetics Conference Exhibition*, Cancun, Mexico. 84–93.
- Epa, 1993. *Geosynthetic Clay Liners (GCLs) in landfill covers*. EPA, Washington, DC, USA, Solid Waste and Emergency Response.
- Epa, 2001. *Geosynthetic Clay Liners used in Municipal Solid Waste Landfills*. EPA, Washington, DC, USA, Solid Waste and Emergency Response.
- Estornell, P., Daniel, D.E., 1992. Hydraulic conductivity of three geosynthetic clay liners. *J. Geotech. Geoenviron. Eng.* 118 (10), 1592–1606.
- Giroud, J.P., Badu-Tweneboah, K., Soderman, K.L., 1997. Comparison of leachate flow through compacted clay liners in landfill liner systems. *Geosynth. Int.* 4 (3–4), 391–431.
- Jo, H.Y., Katsumi, T., Benson, C.H., Edil, T.B., 2001. Hydraulic conductivity and swelling of nonprehydrated GCLs permeated with single-species salt solutions. *J. Geotech. Geoenviron. Eng.* 127 (7), 557–567.
- Jo, H.Y., Benson, C.H., Shackelford, C.D., Lee, J.M., Edil, T.B., 2005. Long-term hydraulic conductivity of a geosynthetic clay liner permeated with inorganic salt solutions. *J. Geotech. Geoenviron. Eng.* 131 (4), 405–417.
- Kendall, P. M., Austin, R. A., 2014. Investigation of GCL overlap techniques using a large scale flow box. 7th Int. Congress on Environmental Geotechnics, International Society of Soil Mechanics and Geotechnical Engineering, London, 746–753.
- Koerner, R. M. 2012. *Designing with Geosynthetics*, 6th Edition, Vol.2, Xlibris Corporation, Bloomington, IN, USA.
- Kolstad, D.C., Benson, C.H., Edil, T.B., 2004. Hydraulic conductivity and swell of nonprehydrated geosynthetic clay liners permeated with multispecies inorganic solutions. *J. Geotech. Geoenviron. Eng.* 130 (12), 1236–1249.
- Li, D., Zainab, B., Tian, K., 2021. Effect of effective stress on hydraulic conductivity of bentonite-polymer geosynthetic clay liners to coal combustion product leachates. *Environmental Geotechnics* 40 (XXXX), 1–12.
- Lee, J.M., Shackelford, C.D., Benson, C.H., Jo, H., Edil, T.B., 2005. Correlating index properties and hydraulic conductivity of geosynthetic clay liners. *J. Geotech. Geoenviron. Eng.* 131 (11), 1319–1329.
- Lu, Y., Abuel-Naga, H., Leong, E.C., Bouazza, A., Lock, P., 2018. Effect of water salinity on the water retention curve of geosynthetic clay liners. *Geotext. Geomembranes* 46 (6), 707–714.
- Mazzieri, F., Di Emidio, G., 2015. Hydraulic conductivity of a denseprehydrated geosynthetic clay liner. *Geosynthetics Int.* 22 (1), 138–148.
- Meer, S.R., Benson, C.H., 2007. Hydraulic conductivity of geosynthetic clay liners exhumed from landfill final covers. *J. Geotech. Geoenviron. Eng.* 133 (5), 550–563.
- Mukunoki, T., Sato, K., Fukushima, J., Shida, K., Take, W.A., 2019. Investigating the mechanism of downslope bentonite erosion in GCL liners using X-Ray CT. *Geotext. Geomembranes* 47 (1), 75–86.
- Parastar, F., Hejazi, S.M., Sheikhzadeh, M., Alirezazadeh, A., 2017. A parametric study on hydraulic conductivity and self-healing properties of geotextile clay liners used in landfills. *J. Environ. Manag.* 202, 29–37.
- Rowe, R.K., Bostwick, L., Thiel, R., 2010. Shrinkage characteristics of heat-tacked GCL seams. *Geotext. Geomembr.* 28 (4), 352–359.
- Rowe, R.K., 2020. Geosynthetic clay liners: Perceptions and misconception. *Geotext. Geomembranes* 48 (2), 137–156.
- Scalia, J., Benson, C.H., 2010. Effect of permeant water on the hydraulic conductivity of exhumed GCLs. *Geotech. Tes J.* 33 (3), 201–211.
- Scalia, J., Benson, C.H., Bohnhoff, G.L., Edil, T.B., Shackelford, C.D., 2014. Long-term hydraulic conductivity of a bentonite-polymer composite permeated with aggressive inorganic solutions. *J. Geotech. Geoenviron. Eng.* 140 (3), 1–13.
- Setz, M.C., Tian, K., Benson, C.H., Bradshaw, S.L., 2017. Effect of ammonium on the hydraulic conductivity of geosynthetic clay liners. *Geotext. Geomembr.* 45, 665–673.
- Shackelford, C.D., Benson, C.H., Katsumi, T., Edil, T.B., Lin, L., 2000. Evaluating the hydraulic conductivity of GCLs permeated with non-standard liquids. *Geotext. Geomembranes* 18 (2–4), 133–161.
- Sharma, H.D., Lewis, S.P., 1994. *Waste containment systems, waste stabilization, and landfills: design and evaluation*. John Wiley & Sons, New York, USA.
- Thiel, R. and Richardson, G.N., 2005. Concern for GCL shrinkage when installed on slopes. In *Geosynthetics Research and Development in Progress* (pp. 1-7).
- Tian, K., Benson, C.H., 2014. Hydraulic conductivity of geosynthetic clay liners exposed to low-level radioactive waste leachate. In *Proc., Waste Management 14*, 1–15. Phoenix: WM Symposia Inc.
- Tian, K., Benson, C.H., Likos, W.J., 2016. Hydraulic conductivity of geosynthetic clay liners to low-level radioactive waste leachate. *J. Geotech. Geoenviron. Eng.* 142 (8), 1–12.
- Tian, K., Likos, W.J., Benson, C.H., 2019. Polymer elution and hydraulic conductivity of bentonite-polymer composite geosynthetic clay liners. *J. Geotech. Geoenviron. Eng.* 145 (10), 1–12.
- Weerasinghe, I., Gallage, C., Dawes, L., Kendall, P., 2020. Factors affecting the hydraulic performance of a geosynthetic clay liner overlap. *J. Environ. Manag.* 271, 110978.
- Zainab, B., Wireko, C., Dong, L., Tian, K., Tarek, K., 2021. Hydraulic conductivity of bentonite-polymer geosynthetic clay liners to coal combustion product leachates. *Geotext. Geomembr.* 49 (5), 1129–1138.